
Degree-Optimized Cumulative Polynomial Kolmogorov-Arnold Networks

Mathew Vanherreweghe
Centre for Quantum Technologies
National University of Singapore
Department of Mathematics
National University of Singapore
v.mathew@u.nus.edu

Lirandë Pira
Centre for Quantum Technologies
National University of Singapore
lpira@nus.edu.sg

Patrick Rebstro
Centre for Quantum Technologies
National University of Singapore
Department of Computer Science
National University of Singapore
cqtfr@nus.edu.sg

Abstract

We introduce cumulative polynomial Kolmogorov-Arnold networks (CP-KAN), a neural architecture combining Chebyshev polynomial basis functions and quadratic unconstrained binary optimization (QUBO). Our primary contribution involves reformulating the degree selection problem as a QUBO task, reducing the complexity from $O(D^N)$ to a single optimization step per layer. This approach enables efficient degree selection across neurons while maintaining computational tractability. The architecture performs well in regression tasks with limited data, showing good robustness to input scales and natural regularization properties from its polynomial basis. Additionally, theoretical analysis establishes connections between CP-KAN's performance and properties of financial time series. Our empirical validation across multiple domains demonstrates competitive performance compared to several traditional architectures tested, especially in scenarios where data efficiency and numerical stability are important. Our implementation, including strategies for managing computational overhead in larger networks is available in Ref. [Authors, 2025].

1 Introduction

Many real-world problems involve complex, high-dimensional functions that are difficult or sometimes impossible to compute exactly. Approximating these functions allows one to make predictions, optimize systems, and analyze data in a computationally feasible way Mhaskar and Pai [2000]; Trefethen [2013]. As such, function approximation plays a fundamental role in virtually any area of science including computational mathematics, machine learning, quantum computing and beyond. Efficient function approximation remains a central challenge in machine learning, particularly in domains requiring high data efficiency and numerical stability [Mitchell, 1997; Bishop, 2006; Murphy, 2022]. While multilayer perceptrons (MLPs) are universal approximators [Cybenko, 1989; Krizhevsky et al., 2012; Simonyan and Zisserman, 2014; LeCun et al., 2015; Goodfellow et al., 2016; He et al., 2016], their application can be hindered by sensitivity to input scaling (requiring normalization) and demands for large datasets [Trihinas et al., 2024]. These limitations motivate

exploring alternative architectures such as Kolmogorov-Arnold networks (KANs) [Liu et al., 2024], inspired by the Kolmogorov-Arnold representation theorem [Kolmogorov, 1956]. Using learnable univariate activation functions on network edges, KANs aim for high expressiveness with potentially greater parameter efficiency than MLPs, showing an initial promise in scientific tasks. To achieve this expressiveness, various KAN architectures have explored different bases, including splines [Liu et al., 2024], wavelets [Bozorgasl and Chen, 2024], and Chebyshev polynomials [Sidharth et al., 2024]. While theoretical work has explored quantum implementations of Chebyshev KANs [Ivashkov et al., 2024], practical classical implementations may face challenges, notably in degree selection.

A crucial challenge with polynomial bases in KANs is selecting the appropriate polynomial degree for each activation function.[Seydi, 2024] The degree choice significantly impacts model expressivity, computational cost, and stability[Ivakhnenko, 1971; Sierra et al., 2001; Park et al., 2004]. Low degrees limit power while high degrees risk overfitting and increase computational overhead.[SS et al., 2024] Different activations may need different degrees, making manual selection or simple heuristics suboptimal. This degree selection is a discrete optimization problem, difficult to integrate into gradient-based training and computationally prohibitive ($O(D^N)$ complexity for N activations and maximum degree D) for exhaustive search [Carpenter et al., 1992; Ghanimi et al., 2024; Li et al., 2024].

To address this challenge, we introduce cumulative polynomial Kolmogorov-Arnold networks (CP-KAN). Our approach uses Chebyshev polynomials and tackles degree selection via quadratic unconstrained binary optimization (QUBO), suitable for discrete optimization [Yarkoni et al., 2022]. We reformulate selecting the optimal degree for each neuron’s polynomial activation as a QUBO problem. This allows efficiently finding optimal degree assignments for all neurons in a layer simultaneously using simulated annealing [Kirkpatrick et al., 1983; D-Wave Systems Inc., 2020; Mo et al., 2021]. This layer-wise QUBO formulation substantially reduces the complexity from the intractable $O(D^N)$ search to a single, feasible optimization step per layer, enabling adaptive structure optimization within the KAN framework[Chen et al., 2023]. The resulting CP-KAN layer architecture is shown in Fig. 1.

Following background in Section 2, Section 3 presents the CP-KAN architecture, detailing its integration of Chebyshev polynomials and our QUBO-based strategy for adaptive degree selection, reducing optimization complexity. This section also connects CP-KAN to financial time series properties. Section 4 provides empirical results, demonstrating the model’s performance and parameter efficiency, particularly in regression. Section 5 analyzes these results, discusses implications and limitations, and suggests future work. Finally, Section 6 summarizes our contributions.

2 Background and Methods

2.1 Kolmogorov-Arnold Networks

Kolmogorov-Arnold networks [Liu et al., 2024] represent a promising architecture for efficient machine learning, building on the foundational Kolmogorov-Arnold representation theorem [Arnold, 1957, 1959]. This theorem establishes that any continuous multivariate function can be represented through compositions of univariate functions. Recent work has shown how quantum resources can enhance KAN implementations through quantum annealing optimization [Yarkoni et al., 2022], particularly when using appropriate basis functions. Specifically, the Kolmogorov-Arnold theorem proves that any continuous function $f : [0, 1]^n \rightarrow \mathbb{R}$ can be expressed as:

$$f(x_1, \dots, x_n) = \sum_{q=0}^{2n} \Phi_q \left(\sum_{p=1}^n \psi_{p,q}(x_p) \right) \quad (1)$$

where Φ_q and $\psi_{p,q}$ are continuous univariate functions [Kolmogorov, 1956]. This representation naturally suggests a neural architecture where inner and outer functions are learned to approximate complex mappings [Liu et al., 2024]. Unlike traditional neural networks that may require significant parameter tuning and large datasets, KANs utilize the Kolmogorov-Arnold theorem to represent complex functions with fewer parameters. While early implementations used b-splines and wavelets [Bozorgasl and Chen, 2024], we focus on Chebyshev polynomials for their orthogonality and efficient spectral convergence for smooth functions.Hu et al. [2021]

2.2 Chebyshev Polynomials and Degree Optimization

The Chebyshev polynomials of the first kind, denoted as $T_n(x)$, form a complete orthogonal basis on $[-1, 1]$ and are defined by the recurrence relation:

$$T_0(x) = 1 \tag{2}$$

$$T_1(x) = x \tag{3}$$

$$T_{n+1}(x) = 2xT_n(x) - T_{n-1}(x) \tag{4}$$

While previous work such as QKAN [Ivashkov et al., 2024] first introduced these polynomials to KAN architectures and explored their quantum implementations, scaling and degree selection remained significant challenges. Our approach makes use of these polynomials in a classical framework optimized for practical applications.

Recent work in efficient architecture optimization [Chen et al., 2023; Sierra et al., 2001; Park et al., 2004] has highlighted the importance of discrete optimization in neural network design. Building on these insights, our primary contribution involves reformulating the polynomial degree selection problem through QUBO optimization, enabling efficient classical implementation while maintaining the theoretical advantages of Chebyshev bases. In our framework, each activation function is defined as:

$$\varphi_{pq}(x) = \frac{1}{d+1} \sum_{r=0}^d w_{pq}^{(r)} T_r(x) \tag{5}$$

where $w_{pq}^{(r)} \in [-1, 1]$ are trainable weights, d is the maximum polynomial degree, and the specific degrees of $T_r(x)$ up to d are selected through our QUBO formulation. Unlike approaches that rely solely on gradient-based optimization [Liu et al., 2023], our classical QUBO formulation enables efficient degree selection while optimizing polynomial combinations across neurons [Chen et al., 2023]. The approach enforces regularization through bounded coefficients, building on advances in binary optimization for neural architecture search [Zhang et al., 2024], applying these techniques specifically to polynomial degree selection and potentially positioning them for future quantum-based optimizations through annealing [Yarkoni et al., 2022] or leveraging Grover-style quantum speedups [Gilliam et al., 2021]. Our implementation can provide practical utility on current hardware. The cumulative polynomial structure further enables representation of hierarchical features, potentially beneficial for financial time series analysis [Dahlhaus, 2012].

3 CP-KAN Architecture and Implementation

3.1 Network Architecture

The CP-KAN framework builds upon the Chebyshev-based Kolmogorov-Arnold framework. At its core lies the KANNeuron, characterized by the triplet (\mathbf{w}, b, d) where $\mathbf{w} \in \mathbb{R}^n$ are projection weights, $b \in \mathbb{R}$ is the projection bias and $d \in \mathbb{N}$ is the polynomial degree which is either QUBO-optimized or fixed. Each neuron implements the following transformation:

$$f(\mathbf{x}) = \sum_{i=0}^d c_i T_i(\alpha(\mathbf{x})), \quad \alpha(\mathbf{x}) = \mathbf{w}^\top \mathbf{x} + b, \tag{6}$$

where T_i denotes the Chebyshev polynomials of the first kind. A CP-KAN layer maps n_{in} inputs to n_{out} outputs through parallel scalar-output neurons, as in Fig. 1. The layer combines these outputs through a learned linear transform, enabling feature interactions. Multiple such layers can be stacked to form a deep CP-KAN architecture.

3.2 Degree Selection Optimization

The challenge of selecting optimal polynomial degrees d_i for each neuron i is a discrete optimization problem, difficult to integrate into gradient descent and computationally prohibitive for exhaustive search. This degree assignment can be formulated as a 0-1 integer program with a one-hot constraint per neuron. For compatibility with quantum and annealing solvers [Yarkoni et al., 2022], we express

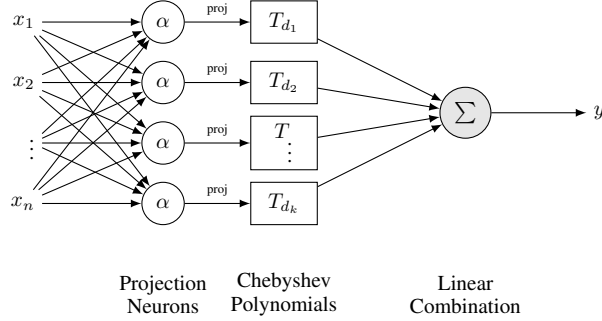


Figure 1: Single layer architecture of CP-KAN showing input features (x_1, \dots, x_n) , projection neurons (α) , Chebyshev polynomial transformations (T_{d_i}) , and their linear combination for output prediction. Each projection neuron learns optimal weights and bias for its input transformation.

it as a QUBO by adding a penalty term for the one-hot constraint. Using binary variables $q_{(i,d)}$ (where $q_{(i,d)} = 1$ when neuron i uses degree d), we create the objective:

$$\min_{\{q_{(i,d)}\} \in \{0,1\}} \left(\sum_{i,d} \text{MSE}_{i,d} \cdot q_{(i,d)} + \alpha \sum_i \left(\sum_d q_{(i,d)} - 1 \right)^2 \right). \quad (7)$$

The first term aims for accurate function approximation through partial least-squares, while the second term enforces a single degree assignment per neuron. A QUBO solver yields optimal degree selections \mathbf{q}^* , after which we determine the polynomial coefficients c_i . See Appendix B for the complete formulation.

3.3 Training Strategy and Two-Phase Optimization

Our training process employs a two-phase strategy combining discrete structure optimization with continuous parameter refinement, designed for hardware agnosticism and potential future quantum readiness [Noy et al., 2020; Kuo et al., 2022]. In Phase 1 (Degree Optimization), the QUBO formulation (Equation (7)) is solved layer-by-layer using simulated annealing to determine the optimal polynomial degree d_i for each neuron i . This phase identifies an effective degree structure. As a practical consideration for large layers where the QUBO problem size $(N \times (D + 1))$ exceeds a threshold T , we may skip QUBO and default to a fixed degree (i.e., $d = 4$) to manage computation, see Algorithm 1. In Phase 2 (Parameter Optimization), following degree selection, all continuous trainable parameters—projection weights \mathbf{w} , biases b , and optionally the polynomial coefficients \mathbf{c} —are fine-tuned using standard gradient-based optimization (i.e., Adam [Kingma and Ba, 2015]) with an appropriate loss function (i.e., MSE or Cross-Entropy) over a set number of epochs. The detailed pseudocode for this process is presented in Algorithm 1 in Appendix C.

3.4 Implementation Considerations

While our QUBO formulation provides a structured approach to degree selection, practical implementation requires careful consideration of computational resources. Memory requirements scale with network size and maximum polynomial degree. Each neuron-degree pair requires storing partial MSE results, creating a memory footprint of shape $(\text{neurons}) \times (\text{max_degree} + 1)$. Solver complexity is tied to the dimension M of the QUBO problem. Our empirical analysis confirms these scaling relationships, with optimization time scaling approximately linearly $O(N)$ with network size N (see Fig. 7). While other optimization methods were explored (see Appendix A), QUBO offered a good balance of performance consistency across domains and computational efficiency, particularly for larger networks. In our implementations, we found problems up to ~ 5000 binary variables $(N \times (D + 1))$ feasible on typical CPU/GPU clusters. Beyond this, alternative strategies such as fixing polynomial degrees for some layers or using the QUBO skipping mechanism (Algorithm 1) provide a balance between optimization quality and computational efficiency.

The effectiveness of CP-KAN, particularly for financial time series, is grounded in its ability to capture locally stationary processes. Chebyshev polynomial basis functions (T_i) are efficient for

representing the smooth, time-varying spectral characteristics ($A_t(\omega)$) inherent in these processes (see Appendix K for details on coefficient decay [Majidian, 2017]). The CP-KAN framework, using QUBO (Sec. 3.2) for adaptive degree selection, gains flexibility to model the complex, evolving dynamics characteristic of local stationarity [Dahlhaus, 2012], learning underlying patterns while adapting to local variations.

4 Experiments

4.1 Datasets Overview

Our analysis utilizes several datasets to evaluate CP-KAN across different tasks. For regression, we use the high-dimensional Jane Street Market Prediction dataset [Desai et al., 2024] and the standard House Price prediction task [Grinsztajn et al., 2022]. For classification, we use MNIST, CIFAR-10, and the Forest Covertype dataset [Grinsztajn et al., 2022]. Full details on data sources, preprocessing, splits, and configurations for each dataset are provided in Appendix D and the respective experimental Appendices C, E, F.

4.2 Model Architectures and Parameter Control

To ensure fair comparisons, all evaluated neural network models (CP-KAN, MLPs) were configured to have approximately the same number of trainable parameters ($\sim 10,000$), controlling for model capacity, unless otherwise stated. Specific architectural choices (i.e., hidden layers, activation functions) and the hyperparameter search spaces used for each dataset are detailed in the corresponding appendices: Jane Street (Appendix E), House Price (Appendix F), MNIST/CIFAR-10 (Appendix G), and Covertype (Appendix H). Baseline models such as RandomForest and XGBoost used standard configurations (Table 12). All models were implemented in PyTorch [Paszke et al., 2019] and trained with the Adam optimizer unless noted otherwise.

4.3 Feature Reshaping for Sequential Models

To adapt sequential models (LSTM, GRU, Transformer) for tabular datasets similar to Jane Street, we employed a feature reshaping technique, treating each feature as an individual step or token in a sequence. This allows standard sequence architectures to process the data. Full implementation details of this embedding trick and the specific recurrent/transformer architectures used are described in Appendix J.

4.4 Financial Market Prediction

The Jane Street Market Prediction task provides a rigorous test of model generalization in a real-world financial context with a custom evaluation metric, defined as:

$$R^2 = 1 - \frac{\sum w_i (y_i - \hat{y}_i)^2}{\sum w_i y_i^2}. \quad (8)$$

where y and \hat{y} denote the vectors of ground-truth and predicted values for the response variable under evaluation, and w is the non-negative sample-weight vector. Our experiments focus on a specific trading window to evaluate performance under limited data conditions. We note that similar results were observed on other trading days with similar data densities. Illustrative training curves showing CP-KAN’s stable convergence compared to MLP on this task can be found here Fig. 3a. To contextualize CP-KAN’s performance, we conducted extensive comparisons against state-of-the-art deep learning architectures widely used for financial time series prediction. We implemented and optimized LSTM, Transformer, and competition-scale GRU models on the Jane Street Market Prediction dataset, as in Appendix J. As shown in Table 2, both CP-KAN variants achieve competitive performance compared to all deep learning models while using orders of magnitude fewer parameters. These R^2 scores, while seemingly low, are highly competitive for this challenging financial prediction task where even small improvements in predictive power can translate to significant trading advantages. Despite employing the feature reshaping technique to optimize performance of sequence-based architectures, CP-KAN still achieved competitive results with fewer parameters. As shown in Table 2, transformers and LSTMs yielded respectable performance but were consistently outperformed by CP-KAN variants with fewer parameters.

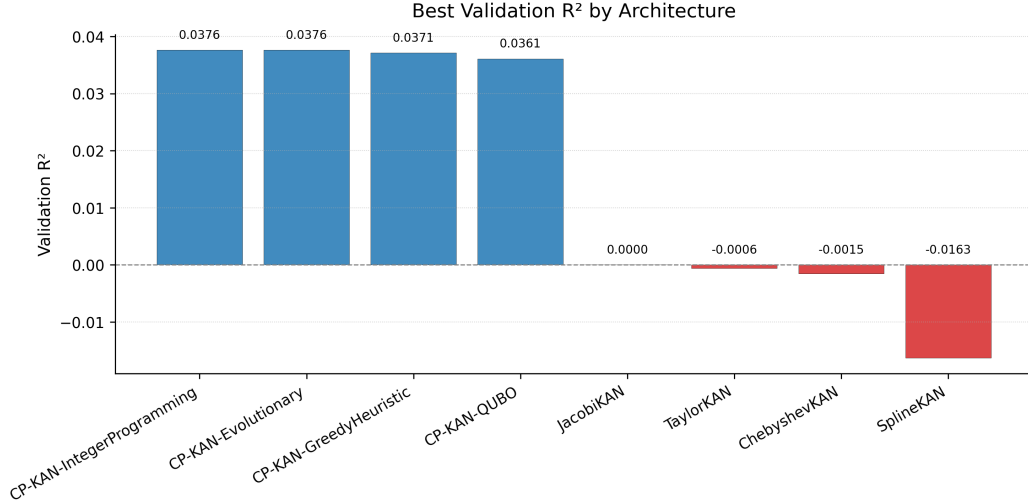
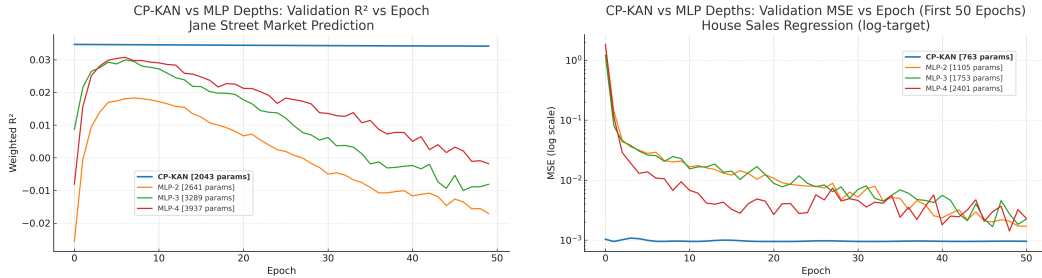


Figure 2: Performance comparison across KAN architectures on the Jane Street Market Prediction dataset. All CP-KAN variants achieve stronger R^2 values than other KAN architectures.



(a) Jane Street dataset: CP-KAN vs. MLP validation performance. (b) House price prediction: CP-KAN vs. MLP training dynamics.

Figure 3: Comparison of training behavior and generalization between CP-KAN and MLPs across two regression tasks. CP-KAN shows more stable and consistent performance.

Our comparative analysis against other KAN architectures as seen in Fig. 2 further validates our approach, with CP-KAN using different optimization methods such as integer programming, greedy heuristic and evolutionary, and 1500–2500 parameters achieved strong results while other polynomial-based KANs fail to exceed mean predictor performance using 6000–9500 parameters after a thorough hyperparameter search. Notably, the standard Chebyshev KAN without our optimization strategy obtained a negative R^2 score, highlighting the importance of the QUBO-based degree selection [Han et al., 2024]. Additionally, ablation studies through hyperparameter grid search finding the best hyperparameters revealed a crucial stability advantage of CP-KAN over traditional architectures for this financial task. As shown in Fig. 4, when the best MLP and KAN models identified by the grid search were trained for additional epochs, MLPs initially achieved competitive performance but exhibited significant performance degradation over extended training periods across multiple learning rates ($1e-5$ to $1e-2$). In contrast, CP-KAN maintained stable and consistent performance throughout, with minimal deviation from peak performance.

4.5 House Price Regression

Our house price prediction experiments suggest CP-KAN’s robustness to input scales, an advantage in real-world regression tasks. The results in Table 1 illustrate this robustness. CP-KAN outperforms MLPs in terms of mean squared errors (MSE) when dealing with raw house prices, indicating stability advantages. This robustness suggests CP-KAN’s potential for handling certain real-world regression tasks without explicit preprocessing. The training dynamic comparison can be found in Fig. 3b).

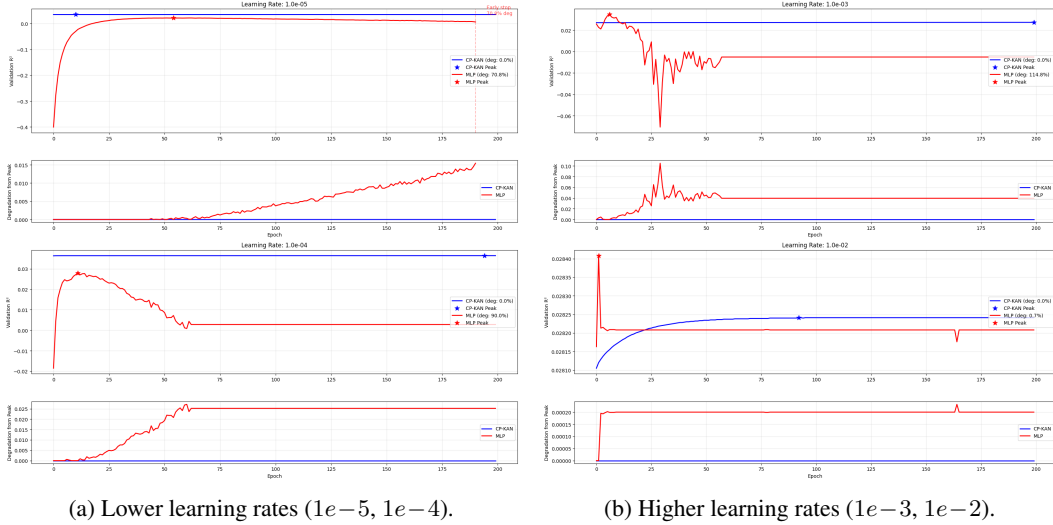


Figure 4: Training stability comparison between MLP and CP-KAN on the Jane Street Market Prediction dataset across varying learning rates.

Table 1: Performance comparison across two tasks: Jane Street market prediction dataset (Validation R^2) and house price prediction dataset (mean squared errors), with observations aligned per task.

Model	Market Prediction: Validation R^2		House Price: Mean Squared Errors (MSE)		
	Validation R^2	Observation	Raw MSE	Log MSE	Observation
CP-KAN (ours)	0.0376	Consistent train-validation performance	0.29	0.0009	Robust to scaling
MLP-4	0.0296	Strong initial performance but unstable, degrades to -0.0042	1823.34	0.0009	Requires normalization
Best Tree Model	0.0293	Strong baseline performance, balancing bias and variance	-	-	-
Random Forest	-	-	0.03	0.0002	Best overall
XGBoost	-	-	0.03	0.0002	Ties RF

5 Experimental Results and Discussion

5.1 Domain-Specific Behavior

Our numerical evaluation indicates CP-KAN’s performance in regression tasks, particularly with limited data and when scale robustness is important. The results suggest stability advantages over traditional neural architectures, supported by its performance on raw house prices without normalization and its resistance to performance degradation in financial time series prediction.

Our comparative analysis offers potential insights into why CP-KAN outperforms traditional deep learning architectures on the tested financial datasets. While our feature reshaping approach (Appendix J) enabled sequence models to process tabular data, these architectures still struggled with generalization. This might relate to optimization difficulties potentially exacerbated by limited data; sequential models may struggle to learn generalizable patterns from fewer examples or converge to suboptimal solutions when processing arbitrarily ordered features [Trihinas et al., 2024; McElfresh et al., 2024; Ren et al., 2025]. The inductive bias of these models assumes sequential relationships, which may not align with the structure of the financial feature vectors tested. In contrast, CP-KAN’s design may be well-suited to the data’s underlying statistical properties, potentially enabling generalization with fewer parameters.

Table 2: Detailed R^2 performance statistics across model architectures on Jane Street (4.4). CP-KAN variants achieve superior performance with dramatically fewer parameters (1, 571 – 2, 547) compared to traditional deep learning models (17, 185 – 506, 701), while significantly outperforming other KAN architectures (6, 693 – 25, 313) despite their larger parameter counts.

Architecture	Mean R^2	Min R^2	Max R^2
CP-KAN-IntegerProgramming (2,547 params)	0.0188	0.0000	0.0376
CP-KAN-Evolutionary (1,571 params)	0.0188	0.0000	0.0376
CP-KAN-GreedyHeuristic (1,571 params)	0.0186	0.0000	0.0371
CP-KAN-QUBO (1,571 params)	0.0241	0.0122	0.0361
Transformer (17,185 params)	0.0345	0.0297	0.0363
LSTM (37,185 params)	0.0312	0.0132	0.0375
GRU Large (506,701 params)	0.0320	0.0144	0.0361
ChebyshevKAN (7,609 params)	-0.4644	-4.6551	-0.0015
JacobiKAN (9,505 params)	-0.6273	-4.0507	-0.0000
SplineKAN (25,313 params)	-0.6985	-4.1313	-0.0163
TaylorKAN (6,693 params)	-0.3540	-3.7172	-0.0006

This domain-dependent behavior suggests a relationship between data characteristics and model stability. In financial time series with high temporal dependency and non-stationarity, MLPs exhibited performance degradation after extended training (Fig. 4a, Fig. 4b), while CP-KAN appeared to maintain consistent performance. This stability gap was less pronounced in housing price prediction (Fig. 3b). The polynomial basis may provide regularization benefits in domains with higher temporal dependency, where traditional architectures may be more prone to overfit transient patterns.

The optimization methods within our CP-KAN framework also exhibit domain-dependent trade-offs. While Integer Programming achieved marginally higher peak performance on financial data, QUBO appeared robust across diverse tasks [Chen et al., 2023]. This cross-domain stability may relate to QUBO’s ability to navigate the discrete optimization landscape while being potentially less susceptible to local minima compared to greedy approaches.

5.2 Parameter Efficiency

CP-KAN resulted in competitive performance with considerably fewer parameters compared to the tested traditional deep learning architectures and other KAN variants (Table 2 and Fig. 2). This efficiency might relate to two key factors: First, the Chebyshev polynomial basis provides an inductive bias potentially suitable for the financial time series tested, capturing underlying dynamics effectively. Second, our QUBO-based degree optimization attempts to match polynomial complexity appropriate for its specific function, avoiding over-parameterization [Sierra et al., 2001; Park et al., 2004].

The performance of CP-KAN in financial time series prompts consideration of why the sequence models, despite their expressive power, did not match CP-KAN’s performance with fewer parameters on this task. One potential explanation is that CP-KAN’s single-feature polynomial transformations may be better suited for the financial data characteristics than the multi-feature learned transformations in other architectures. While sequential models attempt to learn complex dependencies between features treated as sequence steps, they may lack the appropriate inductive bias for the statistical properties of the financial data tested. Additionally, the optimization landscape for such models may be more complex, potentially leading to convergence issues that CP-KAN’s approach potentially avoids.

While the “bigger is better” paradigm drives much of deep learning, this efficiency underscores the continued relevance of tailored architectures with suitable inductive biases for specific domains. CP-KAN’s performance hints that carefully designed, domain-appropriate architectures might outperform generic scaled-up models in certain scenarios. The restricted polynomial degree provides implicit regularization, enhancing parameter efficiency and reducing overfitting risk, especially with limited data. Additionally, the polynomial basis may yield a smoother optimization landscape compared to deeper networks, potentially aiding generalization.

5.3 Theoretical Justification

CP-KAN’s effectiveness for financial time series can be theoretically linked to its ability to capture mean-reverting processes through Chebyshev polynomials. The infinitesimal generator for processes such as the Ornstein-Uhlenbeck SDE admits a Chebyshev expansion (see Appendix K for the formal theorem [Applebaum, 2007]), offering a potential justification for using these polynomials to model financial dynamics. Theoretical error bounds highlight two aspects: an exponential decay term capturing mean reversion, and a term related to polynomial degree showing diminishing returns for higher degrees (Appendix K [Burtnyak and Malys’ka, 2018]). This mathematical foundation helps explain why CP-KAN might capture underlying financial patterns where models lacking this inductive bias might struggle.

5.4 Scaling and Classification

Although CP-KAN was primarily designed for regression tasks, our experiments on MNIST and CIFAR-10 (detailed in Appendix I) indicated scaling properties. The model’s accuracy improved with network width ((Fig. 5b, Fig. 8b)) when QUBO picked lower degrees (Fig. 8b, Fig. 5b) polynomials. Further the QUBO pre-computation time scaled near-linearly ($O(N)$) as shown in Fig. 7. These findings suggest that CP-KAN might potentially overcome its limitations for classification tasks without prohibitive computational overhead. However, CP-KAN’s reliance on smooth polynomials appears to be a challenge for classification tasks requiring sharp decision boundaries, as seen in the Forest Covertype dataset (configuration in Appendix H) where tree-based methods significantly outperformed it (Appendix I.3). This limitation aligns with theoretical expectations that polynomial bases struggle to approximate the necessary discontinuities effectively. While CP-KAN may require increased width for competitive classification performance, it may achieve this scaling more efficiently than traditional architectures due to its polynomial basis and adaptive degree selection. Rather than uniformly scaling all parameters, CP-KAN’s QUBO optimization allows selective complexity increases where needed, offering a nuanced approach to scaling in neural network design.

6 Conclusion

This work presented CP-KAN, a cumulative Kolmogorov-Arnold polynomial network, illustrating how the classical polynomial approximation theory could be combined with neural architectures through adaptive degree selection. By reformulating the choice of polynomial degree as a QUBO optimization problem solved via simulated annealing, we observed competitive performance in regression tasks, particularly for financial time-series prediction. Our empirical results indicate that CP-KAN achieves competitive performance with considerably fewer parameters compared to the tested traditional deep learning architectures. Although challenges remain, notably the classification performance gap and computational overhead for very large networks, our results suggest that polynomial-based neural architectures could be a viable direction for certain real-world regression tasks.

The CP-KAN framework opens several research directions. First, the polynomial basis offers opportunities for efficient online updates, where coefficients could be adapted as new financial data arrives while maintaining theoretical guarantees. Second, the complementary strengths of polynomials (smooth function approximation) and decision trees (discrete boundaries) suggest hybrid models combining CP-KAN’s regression capabilities with tree-based mechanisms, potentially addressing the classification limitations. Additionally, while our current approach selects degrees once, an adaptive system could evolve degrees during training, leading to architectures that adjust complexity to local feature importance [Kuo et al., 2022]. The connection between QUBO optimization and polynomial degree selection also suggests avenues for further theoretical study regarding optimized polynomial bases. Finally, advanced optimization techniques such as quantum annealing could offer a framework for optimizing network parameters [Hauke et al., 2020], with the adiabatic theorem suggesting potential pathways for exploring the optimization landscape [Albash and Lidar, 2018]. CP-KAN represents an architectural approach toward potentially more principled and efficient neural networks. As machine learning evolves, approaches that blend classical mathematical insights with modern optimization techniques may prove valuable, demonstrating how revisiting fundamental approximation theory through the lens of contemporary machine learning might yield practical benefits and theoretical understanding.

Acknowledgments. This work is supported by the National Research Foundation, Singapore, and A*STAR under its CQT Bridging Grant and its Quantum Engineering Programme under grant NRF2021-QEP2-02-P05.

References

- Tameem Albash and Daniel A Lidar. Adiabatic quantum computation. *Reviews of Modern Physics*, 90(1):015002, 2018.
- David Applebaum. On the infinitesimal generators of ornstein–uhlenbeck processes with jumps in hilbert space. *Potential Analysis*, 26:79–100, 2007. URL <https://api.semanticscholar.org/CorpusID:34118491>.
- Vladimir Arnold. On functions of three variables. *Dokl. Akad. Nauk SSSR*, 114:679–681, 1957. URL https://doi.org/10.1007/978-3-642-01742-1_2.
- Vladimir Arnold. On the representation of continuous functions of three variables by superpositions of continuous functions of two variables. *Mat. Sb. (N.S.)*, 48(90)(1):3–74, 1959. URL https://doi.org/10.1007/978-3-642-01742-1_6.
- CP-KAN Authors. CP-KAN Implementation. <https://github.com/Mathewvanh/CP-KAN>, 2025. Accessed: 2025-05-18.
- Christopher M. Bishop. *Pattern Recognition and Machine Learning (Information Science and Statistics)*. Springer-Verlag, Berlin, Heidelberg, 2006. ISBN 978-0-387-31073-2.
- Z. Bozorgasl and H. Chen. Wav-kan: Wavelet kolmogorov-arnold networks. *arXiv preprint arXiv:2405.12832*, 2024.
- Ivan Burtnyak and H. P. Malys’ka. Application of the spectral theory and perturbation theory to the study of ornstein-uhlenbeck processes. *Carpathian Mathematical Publications*, 2018. URL <https://api.semanticscholar.org/CorpusID:126571180>.
- Gail A. Carpenter, Stephen Grossberg, Natalya Markuzon, Joseph H. Reynolds, and David B. Rosen. Artmap: Supervised real-time learning and classification of nonstationary data. *Neural Networks*, 5(6):565–588, 1992.
- Xin Chen, Donglin Zhou, and Zhanxing Wang. Efficient neural architecture search via discrete optimization. *IEEE Transactions on Pattern Analysis and Machine Intelligence*, 45(8):9571–9585, 2023.
- George Cybenko. Approximation by superpositions of a sigmoidal function. *Math. Control Signals Syst.*, 2(4):303–314, 1989. URL <https://doi.org/10.1007/BF02551274>.
- D-Wave Systems Inc. Neal: A python module for optimizing binary quadratic models using simulated annealing, 2020. URL <https://github.com/dwavesystems/dwave-neal>.
- Rainer Dahlhaus. Locally stationary processes. *Handbook of Statistics*, 30:351–413, 2012.
- Maanit Desai, Yirun Zhang, Ryan Holbrook, Kait O’Neil, and Maggie Demkin. Jane street real-time market data forecasting. <https://kaggle.com/competitions/jane-street-real-time-market-data-forecasting>, 2024. Kaggle.
- Hayder M. A. Ghanimi, T. Gopalakrishnan, G. Joel Sunny Deol, K. Amarendra, Pankaj Dadheech, and Sudhakar Sengan. Chebyshev polynomial approximation in cnn for zero-knowledge encrypted data analysis. *Journal of Discrete Mathematical Sciences and Cryptography*, 2024. URL <https://api.semanticscholar.org/CorpusID:268980914>.
- Austin Gilliam, Stefan Woerner, and Constantin Gonciulea. Grover Adaptive Search for Constrained Polynomial Binary Optimization. *Quantum*, 5:428, April 2021. ISSN 2521-327X. doi: 10.22331/q-2021-04-08-428. URL <https://doi.org/10.22331/q-2021-04-08-428>.
- Ian Goodfellow, Yoshua Bengio, and Aaron Courville. *Deep Learning*. MIT Press, 2016. URL <https://www.deeplearningbook.org>.

- Leo Grinsztajn, Edouard Oyallon, and Gael Varoquaux. Why do tree-based models still outperform deep learning on typical tabular data? In S. Koyejo, S. Mohamed, A. Agarwal, D. Belgrave, K. Cho, and A. Oh, editors, *Advances in Neural Information Processing Systems*, volume 35, pages 507–520. Curran Associates, Inc., 2022. URL https://proceedings.neurips.cc/paper_files/paper/2022/file/0378c7692da36807bdec87ab043cdadc-Paper-Datasets_and_Benchmarks.pdf.
- Xiao Han, Xinfeng Zhang, Yiling Wu, Zhenduo Zhang, and Zhe Wu. Kan4tsf: Are kan and kan-based models effective for time series forecasting? In *arXiv*, 2024.
- Philipp Hauke, Helmut G Katzgraber, Wolfgang Lechner, Hidetoshi Nishimori, and William D Oliver. Perspectives of quantum annealing: Methods and implementations. *Reports on Progress in Physics*, 83(5):054401, 2020.
- Kaiming He, Xiangyu Zhang, Shaoqing Ren, and Jian Sun. Deep residual learning for image recognition. In *2016 IEEE Conference on Computer Vision and Pattern Recognition (CVPR)*, pages 770–778, 2016. URL <https://doi.org/10.1109/CVPR.2016.90>.
- Jingwei Hu, Xiaodong Huang, Jie Shen, and Haizhao Yang. A fast petrov-galerkin spectral method for the multi-dimensional boltzmann equation using mapped chebyshev functions, 2021. URL <https://arxiv.org/abs/2105.08806>.
- A. G. Ivakhnenko. Polynomial theory of complex systems. *IEEE Transactions on Systems, Man, and Cybernetics*, SMC-1(4):364–378, 1971.
- Petr Ivashkov, Po-Wei Huang, Kelvin Koor, Lirandë Pira, and Patrick Reberntrost. Qkan: Quantum kolmogorov-arnold networks, 2024. URL <https://arxiv.org/abs/2410.04435>.
- Diederik P. Kingma and Jimmy Ba. Adam: A method for stochastic optimization. In *3rd International Conference on Learning Representations (ICLR)*, 2015. URL <https://arxiv.org/abs/1412.6980>.
- S. Kirkpatrick, C. D. Gelatt Jr, and M. P. Vecchi. Optimization by simulated annealing. *Science*, 220(4598):671–680, 1983. doi: 10.1126/science.220.4598.671. URL <https://doi.org/10.1126/science.220.4598.671>.
- Andrey Kolmogorov. On the representation of continuous functions of several variables by superpositions of continuous functions of a smaller number of variables. *Dokl. Akad. Nauk SSSR*, 108:179–182, 1956. URL <https://cs.uwaterloo.ca/~y328yu/classics/Kolmogorov56.pdf>.
- Alex Krizhevsky, Ilya Sutskever, and Geoffrey E Hinton. Imagenet classification with deep convolutional neural networks. In *Advances in Neural Information Processing Systems*, volume 25, pages 1097–1105. Curran Associates, Inc., 2012.
- Chun Lin Kuo, Ercan Engin Kuruoglu, and Wai Kin Victor Chan. Neural network structure optimization by simulated annealing. *Entropy*, 24(3), 2022. ISSN 1099-4300. doi: 10.3390/e24030348. URL <https://www.mdpi.com/1099-4300/24/3/348>.
- Yann LeCun, Yoshua Bengio, and Geoffrey Hinton. Deep learning. *Nature*, 521(7553):436–444, 2015. URL <https://doi.org/10.1038/nature14539>.
- Shaozhi Li, M Sabbir Salek, Yao Wang, and Mashrur Chowdhury. Quantum-inspired activation functions and quantum chebyshev-polynomial network, 2024. URL <https://arxiv.org/abs/2404.05901>.
- Hangyu Liu, Gabriel Bender, Yichen Sun, Alvin Wan, Ruihan Yang, and Kevin Swersky. Gradient-free neural architecture search via zero-cost proxies. *arXiv preprint arXiv:2301.05787*, 2023.
- Ziming Liu, Yixuan Wang, Sachin Vaidya, Fabian Ruehle, James Halverson, Marin Soljačić, Thomas Y. Hou, and Max Tegmark. KAN: Kolmogorov-Arnold networks, 2024.
- Hassan Majidian. On the decay rate of chebyshev coefficients. *Applied Numerical Mathematics*, 113:44–53, 11 2017. doi: 10.1016/j.apnum.2016.11.004.

- Duncan McElfresh, Sujay Khandagale, Jonathan Valverde, Vishak Prasad C, Benjamin Feuer, Chinmay Hegde, Ganesh Ramakrishnan, Micah Goldblum, and Colin White. When do neural nets outperform boosted trees on tabular data?, 2024. URL <https://arxiv.org/abs/2305.02997>.
- Hrushikesh Narhar Mhaskar and Devidas V. Pai. *Fundamentals of Approximation Theory*. CRC Press, 2000. ISBN 978-0-8493-0939-7.
- Yanhui Mi. A modified stochastic volatility model based on gamma ornstein–uhlenbeck process and option pricing, 2016. URL <https://api.semanticscholar.org/CorpusID:156849598>.
- Tom M. Mitchell. *Machine Learning*. McGraw-Hill, New York, 1997. ISBN 9780070428072.
- Shentong Mo, Jingfei Xia, and Pinxu Ren. Simulated annealing for neural architecture search. In *Workshop on Optimization for Machine Learning (OPT) at NeurIPS 2021*, Pittsburgh, PA, USA, 2021.
- Kevin P. Murphy. *Machine Learning: A Probabilistic Perspective*. MIT Press, Cambridge, MA, 2 edition, 2022. ISBN 9780262046824.
- Asaf Noy, Niv Nayman, Tal Ridnik, Nadav Zamir, Sivan Doveh, Itamar Friedman, Raja Giryes, and Lihi Zelnik-Manor. Asap: Architecture search, anneal and prune. In *International Conference on Artificial Intelligence and Statistics*, pages 1266–1276. PMLR, 2020.
- Ho-Sung Park, Byoung-Jun Park, Hyun-Ki Kim, and Sung-Kwun Oh. Self-organizing polynomial neural networks based on genetically optimized multi-layer perceptron architecture. *International Journal of Control, Automation, and Systems*, 2(4):423–434, 2004.
- Adam Paszke et al. Pytorch: An imperative style, high-performance deep learning library. In *Advances in Neural Information Processing Systems 32*, pages 8024–8035, 2019. URL <https://arxiv.org/abs/1912.01703>.
- Weijieying Ren, Tianxiang Zhao, Yuqing Huang, and Vasant Honavar. Deep learning within tabular data: Foundations, challenges, advances and future directions, 2025. URL <https://arxiv.org/abs/2501.03540>.
- Seyd Teymoor Seydi. Exploring the potential of polynomial basis functions in kolmogorov-arnold networks: A comparative study of different groups of polynomials, 2024. URL <https://arxiv.org/abs/2406.02583>.
- S.S. Sidharth, A.R. Keerthana, R. Gokul, and K.P. Anas. Chebyshev polynomial-based Kolmogorov-Arnold networks: An efficient architecture for nonlinear function approximation, 2024.
- Alejandro Sierra, José Macías, and Fernando Corbacho. Evolution of functional link networks. *Evolutionary Computation, IEEE Transactions on*, 5:54 – 65, 03 2001. doi: 10.1109/4235.910465.
- Karen Simonyan and Andrew Zisserman. Very deep convolutional networks for large-scale image recognition. *arXiv preprint arXiv:1409.1556*, 2014.
- Sidharth SS, Keerthana AR, Gokul R, and Anas KP. Chebyshev polynomial-based kolmogorov-arnold networks: An efficient architecture for nonlinear function approximation, 2024. URL <https://arxiv.org/abs/2405.07200>.
- Lloyd N. Trefethen. *Approximation Theory and Approximation Practice*. Society for Industrial and Applied Mathematics, Philadelphia, PA, 2013. ISBN 978-1-611972-39-9.
- Demetris Trihinas, Panagiotis Michael, and Moysis Symeonides. Evaluating dl model scaling trade-offs during inference via an empirical benchmark analysis. *Future Internet*, 2024. URL <https://api.semanticscholar.org/CorpusID:274805777>.
- S. Yarkoni, E. Raponi, T. Bäck, and S. Schmitt. Quantum annealing for industry applications: introduction and review. *Rep. Prog. Phys.*, 85:104001, 2022.
- Yuge Zhang, Yufan Wang, Ruizhe Yang, and Lei Li. Binary neural architecture search with high performance computing. *IEEE Transactions on Neural Networks and Learning Systems*, 35(1): 711–723, 2024.

Computational Environment: All experiments reported in these appendices were performed on an Apple MacBook Pro (Late 2021) with an M1 Pro chip and 16GB of RAM. With the exception of the LSTM, GRU, Transformer experiments ran on a single H100 GPU.

Appendix

A Optimization Methods

This section details the mathematical formulation of the different polynomial degree selection methods implemented for the CP-KAN architecture. For a given KAN layer with N_{in} inputs and N_{out} neurons, the goal is to select a degree $d_i \in \{0, 1, \dots, D_{\text{max}}\}$ for each neuron $i = 0, \dots, N_{\text{out}} - 1$. Let $\mathbf{X} \in \mathbb{R}^{B \times N_{\text{in}}}$ be the input data batch and $\mathbf{Y} \in \mathbb{R}^{B \times N_{\text{out}}}$ be the target data for this layer (either the final targets or dimension-aligned intermediate targets). Let $\mathbf{y}_i \in \mathbb{R}^B$ be the target vector for the i -th neuron. Let $T_d(\alpha)$ denote the Chebyshev polynomial of the first kind of degree d , evaluated at α . For the i -th neuron, the projection is $\alpha_i = \mathbf{w}_i \mathbf{X} + b_i$. The cumulative transform up to degree d produces a matrix $\Phi_{i,d} \in \mathbb{R}^{B \times (d+1)}$ where the k -th column is $T_k(\alpha_i)$. The least-squares coefficients for fitting \mathbf{y}_i with degree d are:

$$\mathbf{c}_{i,d} = (\Phi_{i,d}^\top \Phi_{i,d})^{-1} \Phi_{i,d}^\top \mathbf{y}_i,$$

and the resulting prediction is:

$$\hat{\mathbf{y}}_{i,d} = \Phi_{i,d} \mathbf{c}_{i,d}.$$

The MSE for neuron i with degree d is defined as:

$$\text{MSE}_{i,d} = \frac{1}{B} \|\mathbf{y}_i - \hat{\mathbf{y}}_{i,d}\|_2^2.$$

B Quadratic Unconstrained Binary Optimization (QUBO) Formulation for Degree Selection

We start by selecting the optimal polynomial degree for each neuron to minimize the total mean squared error while enforcing that exactly one degree is chosen per neuron. We use binary variables $x_{i,d} \in \{0, 1\}$, where $x_{i,d} = 1$ if neuron i uses degree d , and 0 otherwise. These values can be summarized in a Boolean matrix X . This problem can be expressed as:

$$\min_{x_{i,d} \in \{0,1\}} \sum_{i=1}^N \sum_{d=0}^D c_{i,d}(X) x_{i,d}, \quad (9)$$

$$\text{subject to: } \sum_{d=0}^D x_{i,d} = 1 \quad \forall i, \quad (10)$$

$$x_{i,d} \in \{0, 1\} \quad \forall i, d \quad (11)$$

where $c_{i,d}$ represents the MSE cost when neuron i uses degree d , N is the number of neurons, and D is the maximum degree allowed. Using binary variables $q_{(i,d)}$ (equivalent to $x_{i,d}$), we eliminate explicit constraints by incorporating them as penalty terms:

$$\min_{\{q_{(i,d)}\} \in \{0,1\}} \underbrace{\left(\sum_{i,d} \text{MSE}_{i,d} \cdot q_{(i,d)} \right)}_{\text{fidelity cost}} + \underbrace{\alpha \sum_i \left(\sum_d q_{(i,d)} - 1 \right)^2}_{\text{one-hot penalty}} \quad (12)$$

The problem is solved using a QUBO solver (e.g., simulated annealing) to find the binary assignment $\{q_{(i,d)}\}$ that minimizes the objective. The degree d for which $q_{(i,d)} = 1$ is selected for neuron i , and the corresponding pre-computed coefficients $\mathbf{c}_{i,d}$ are assigned. This QUBO formulation enables efficient degree selection while maintaining compatibility with both classical simulated annealing and quantum annealing hardware.

B.1 Integer Programming (IP)

The integer programming formulation minimizes the MSE for each neuron independently using a mixed integer linear programming (MILP) solver. For each neuron i , binary variables $x_{i,d} \in \{0, 1\}$, where $x_{i,d} = 1$ if neuron i uses degree d , and 0 otherwise. The Objective function (for each neuron i) is :

$$\text{Minimize } \sum_{d=0}^{D_{\max}} \text{MSE}_{i,d} \cdot x_{i,d}$$

with constraint (for each neuron i):

$$\sum_{d=0}^{D_{\max}} x_{i,d} = 1$$

The MILP problem is solved independently for each neuron i using a solver like OR-Tools SCIP. The degree d for which $x_{i,d} = 1$ is selected, and the corresponding coefficients $\mathbf{c}_{i,d}$ are assigned.

B.2 Evolutionary Algorithm (EA)

The Evolutionary Algorithm leverages principles of natural selection to efficiently determine an optimal combination of polynomial degrees for all neurons within a given layer simultaneously. Each individual within the algorithm’s population is represented by a vector of degrees $\mathbf{d} = [d_0, d_1, \dots, d_{N_{\text{out}}-1}]$, where each degree d_i can take integer values from 0 up to a predefined maximum degree D_{\max} . The fitness of each individual \mathbf{d} is calculated as the sum of the mean squared errors for each neuron when using the degrees specified by that individual:

$$\text{Fitness}(\mathbf{d}) = \sum_{i=0}^{N_{\text{out}}-1} \text{MSE}_{i,d_i}.$$

The process begins with the initialization of a random population of individuals. For a fixed number of generations, the algorithm performs the following steps: First, it evaluates the fitness of each individual. Then, parents are selected based on their fitness scores, typically favoring those with lower fitness values. Offspring are generated using genetic operators such as crossover, where segments of two parent individuals’ degree vectors are combined (for instance, through single-point crossover), and mutation, which involves randomly altering a degree value with a small probability. Optionally, elitism may be applied by preserving one or more of the top-performing individuals from the current generation into the next, ensuring that the best solutions found are not lost. The newly formed offspring then replace the previous population, constituting the new generation. Finally, after completing the predetermined number of generations, the algorithm selects the individual with the lowest fitness as the optimal solution. The degrees from this best individual are then assigned to their respective neurons along with the corresponding pre-computed coefficients \mathbf{c}_{i,d_i} .

B.3 Greedy Heuristic

The Greedy Heuristic optimization strategy determines the polynomial degree for each neuron sequentially, layer by layer. For a given neuron i in a layer, the algorithm iterates through possible degrees $d = 0, 1, \dots, D_{\max}$. For each candidate degree d , it computes the Chebyshev basis functions $\Phi_{i,d}$ based on the layer’s input data and calculates the optimal least-squares coefficients $\mathbf{c}_{i,d}$ to predict the neuron’s target \mathbf{y}_i (either the final task target for the output layer or a dimension-aligned intermediate target for hidden layers, as described in Appendix A). The corresponding Mean Squared Error, $\text{MSE}_{i,d}$, is calculated.

The algorithm tracks the degree d^* that yields the lowest MSE encountered so far. A key feature is an early stopping mechanism: the iteration over degrees for neuron i terminates prematurely if the relative improvement in MSE from degree $d - 1$ to d , defined as $(\text{MSE}_{i,d-1} - \text{MSE}_{i,d}) / \text{MSE}_{i,d-1}$, falls below a predefined `improvement_threshold` (e.g., 1%). Once the iteration stops (either by reaching D_{\max} or triggering early stopping), the neuron i is assigned the best degree d^* found and its corresponding coefficients \mathbf{c}_{i,d^*} . The process then repeats for the next neuron in the layer. After all neurons in the current layer are optimized, their outputs are computed and passed as input to the subsequent layer. The configuration option `skip_qubo_for_hidden` (though named historically) can bypass this optimization for hidden layers, setting them to a default degree instead.

C CP-KAN Training Algorithm Details

This appendix provides the detailed pseudocode for the two-phase training strategy discussed in Section 3.

Algorithm 1 CP-KAN Training Algorithm

Require: Train/val data $(X_{train}, y_{train}), (X_{val}, y_{val})$, network shape, max degree D , QUBO threshold T , learning rate η , epochs E

Ensure: Trained CP-KAN model

- 1: Initialize CP-KAN model \mathcal{M} with random weights and biases
- Phase 1: Degree Optimization via QUBO**
- 2: **for** layer $l = 1$ to L **do**
- 3: Set all neurons to degree 3 if $N_l \times (D + 1) > T$ ▷ Skip large layers
- 4: **if** $N_l \times (D + 1) \leq T$ **then**
- 5: Compute MSE costs $c_{i,d}$ for each neuron-degree pair (Appendix B)
- 6: Construct QUBO matrix Q with costs and one-hot penalties
- 7: $\mathbf{q}^* \leftarrow$ Solve QUBO using simulated annealing
- 8: Set layer l degrees according to solution \mathbf{q}^*
- 9: **end if**
- 10: **end for**
- Phase 2: Parameter Optimization**
- 11: Collect trainable params $\Theta = \{(\mathbf{w}, b, c)\}$ for all neurons
- 12: Initialize Adam optimizer with learning rate η
- 13: **for** epoch $e = 1$ to E **do**
- 14: Compute loss $\mathcal{L} \leftarrow \text{Loss}(\mathcal{M}(X_{train}), y_{train})$ ▷ e.g., MSE or CrossEntropy
- 15: Update parameters Θ using Adam
- 16: Monitor validation loss for early stopping (if applicable)
- 17: **end for**
- 18: **return** Trained model \mathcal{M}

D Data Preprocessing and Configuration

D.1 Jane Street Dataset Configuration

For the Jane Street Market Prediction dataset, preprocessing involved selecting 79 numeric features (feature 00 through feature 78). Samples were weighted according to a specified column, aligning with the competition’s weighted evaluation metrics (weighted MSE and weighted R²). The dataset also included date-based information (date id) to facilitate temporal analysis or validation splits. Experiments typically employed a train-validation split of 70% training and 30% validation data. To manage computational resources effectively, a subset of 200,000 rows was commonly used.

Table 3: Jane Street Dataset Configuration

Parameter	Value
Data Path	(Kaggle Jane Street Market Prediction dataset path)
Rows Used	200,000
Train Ratio	0.7
Feature Columns	feature_00 through feature_78 (79 features)
Target Column	'responder_6'
Weight Column	'weight'
Date Column	'date_id'

D.2 House Sales Dataset Configuration

For the House Sales regression dataset, data was loaded from “inria-soda/tabular-benchmark” (reg_num/house_sales.csv). The target variable (housing prices) was log-transformed using `np.log1p()` to reduce skewness and improve model training stability. Features were normalized using `StandardScaler()` to ensure zero mean and unit variance. For experimentation, 80% of data was used for training and 20% for validation, with a fixed random seed of 42.

D.3 Covertypes Dataset Configuration

For the Covertypes classification dataset, data was loaded from “inria-soda/tabular-benchmark” (clf_num/covertypes.csv). The class labels were extracted from the “target” column (or the last column if named differently). A train-validation split of 80% – 20% was implemented with a fixed random seed of 42.

D.4 MNIST and CIFAR-10 Configurations

For the image classification datasets:

- **MNIST:** Standard normalization with mean 0.1307 and std 0.3081 was applied. Images were flattened from 2828 to 784-dimensional input vectors.
- **CIFAR-10:** Standard normalization with mean (0.5, 0.5, 0.5) and std (0.5, 0.5, 0.5) was applied. Images were flattened from 3×32×32 to 3072-dimensional input vectors.
- **Batch Size:** 64 was used as the standard batch size for both datasets.
- **Training:** Models used CrossEntropy loss and targets were converted to one-hot format for QUBO optimization.

E Hyperparameter Configurations for Jane Street Experiments

E.1 Experiment 1: CP-KAN Optimization Method Comparison

This experiment compared the performance of different degree optimization strategies within the CP-KAN framework. A grid search was performed across various architectural and training hyperparameters, applying the same grid to each optimization method tested.

Table 4: Hyperparameter Grid Search for CP-KAN Optimization Methods (Jane Street)

Hyperparameter	Values Searched
Optimization Methods Tested	QUBO, IntegerProgramming, Evolutionary, GreedyHeuristic
Grid Search Parameters (Applied to all methods):	
Max Degree	{3, 5, 7, 9}
Hidden Size	{16, 20, 24, 32}
Hidden Degree	{3, 5, 7}
Learning Rate	{1e-2, 5e-3, 1e-3}

E.2 Experiment 2: CP-KAN vs MLP Architecture Comparison

This experiment performed a grid search to compare the performance of the CP-KAN architecture against various MLP architectures (see Table 5). The goal was to find suitable base configurations for further analysis, such as the stability tests in Experiment 3.

Table 5: Hyperparameter Grid Search for KAN vs MLP (Jane Street – Pre-Degradation)

Model	Hyperparameter	Values Searched
CP-KAN	Max Degree	{5, 7, 9}
	Hidden Size	{16, 20, 24, 28}
	Hidden Degree	{3, 5, 7}
	Learning Rate	{0.01, 0.005}
MLP	Hidden Size	{20, 24, 28}
	Depth	{2, 3, 4}
	Dropout	{0.1, 0.15}
	Learning Rate	{0.01, 0.005}

E.3 Experiment 3: Training Stability / Degradation Analysis

This experiment investigated the training stability and performance degradation using the best performing CP-KAN and MLP configurations identified from Experiment 2 (Table 5). These chosen architectures (CP-KAN with 20 hidden neurons; MLP with hidden size 24 and depth 3) were then trained with different learning rates to observe stability patterns. The specific fixed parameters for these chosen models are detailed in Table 6.

Table 6: Fixed Configurations (Best from Exp. 2) for Degradation Analysis (Jane Street)

Model	Parameter	Fixed Value
CP-KAN	Network Shape	[Input Dim, 20 , 1]
	Max Degree	5
	Complexity Weight	0.0
	Trainable Coefficients	True
	Skip QUBO for Hidden	False
	Default Hidden Degree	5
MLP	Hidden Size	24
	Depth	3
	Dropout Rate	0.1 (default in build_mlp)
Variable Parameter for this Experiment:		
KAN & MLP	Learning Rate	{1e-2, 1e-3, 1e-4, 1e-5}

E.4 Experiment 4: Hyperparameter Grids for KAN Architecture Comparison (Jane Street)

This experiment compared various KAN architectures against each other and other models like MLPs on the Jane Street dataset. The following hyperparameter grids were searched for each model type. Note that CP-KAN variants shared a similar grid structure. The base `learning_rate` for training loops was 1e-3, but could be overridden by specific model configurations if included in their grid search.

F Hyperparameter Grid Search for House Sales Dataset

This experiment performed a hyperparameter grid search comparing CP-KAN and MLP architectures on the House Sales regression dataset (using log-transformed target values).

G Optimization Method Evaluation (MNIST, CIFAR-10)

This experiment aimed to compare different CP-KAN optimization methods (QUBO, IntegerProgramming, Evolutionary, GreedyHeuristic) using a hyperparameter grid search. The target datasets were MNIST and CIFAR-10, though the execution was adapted based on initial results on MNIST. On MNIST, the IntegerProgramming, Evolutionary, and GreedyHeuristic methods yielded near-random accuracy ($\approx 11.35\%$), while QUBO achieved significantly better performance (37.48% accuracy). Due to the poor results from the other methods on MNIST, the planned grid search was **not** conducted for them on CIFAR-10.

Where applicable, base training parameters such as `num_epochs` were set to 50. The hyperparameter grid search was applied as follows:

- **MNIST:** All four methods (QUBO, IP, Evo, Greedy) were evaluated using the full grid. Only QUBO demonstrated promising results.
- **CIFAR-10:** Only QUBO was evaluated using the grid search. A few runs with IP configurations were attempted, but yielded worse-than-random performance ($\approx 9\%$ accuracy).

Table 7: Hyperparameter Grid Search for KAN Architecture Comparison

Model Type	Hyperparameter	Values Searched
CP-KAN (All variants)	Max Degree	{5, 7, 9}
	Complexity Weight	{0.05, 0.1, 0.2}
	Trainable Coefficients	{False, True}
	Skip QUBO for Hidden	{False, True}
	Default Hidden Degree	{3, 4, 5}
	Hidden Dims	[20] (Fixed)
Original-KAN (Spline)	Hidden Dim	{16, 20, 24, 32}
	Num (Spline Intervals)	{3, 5, 7}
	K (Spline Order)	{2, 3, 4}
Wavelet-KAN	Hidden Dim	{16, 20, 24, 32}
	With Batch Norm	{True, False}
	Wavelet Type	'mexican_hat' (Fixed)
Jacobi-KAN	Hidden Dim	{16, 20, 24, 32}
	Degree	{3, 5, 7}
	Parameter a	{0.5, 1.0, 1.5}
	Parameter b	{0.5, 1.0, 1.5}
Chebyshev-KAN (ChebyKAN)	Hidden Dim	{16, 20, 24, 32}
	Degree	{3, 5, 7, 9}
Taylor-KAN	Hidden Dim	{16, 20, 24, 32}
	Order	{2, 3, 4, 5}
	Add Bias	True (Fixed)
RBF-KAN	Hidden Dim	{16, 20, 24, 32}
	Num Centers	{5, 10, 15, 20}
	Alpha (Shape Param)	{0.5, 1.0, 2.0}
MLP	Hidden Dims	[32], [64], [128], [32, 32], [64, 64]
	Dropout	{0.1, 0.2, 0.3}
	Use Batch Norm	{True, False}

H Covertypes Classification Configuration

This experiment compared CP-KAN against an MLP on the Covertypes classification dataset (`test_tabular_data.py`). The KAN and MLP architectures were automatically configured to target a similar parameter count (`desired_params = 10000`), rather than using a grid search. Standard RandomForest and XGBoost models were also trained as baselines using fixed configurations.

I Scaling and Classification Benchmarks

I.1 MNIST Benchmark

To provide further insight into the scaling properties of CP-KAN and the comparison between optimization methods, we present additional results from experiments conducted on the MNIST dataset. These results parallel the analysis performed on CIFAR10 in the main text. Fig. 5a shows the impact of varying the maximum allowed polynomial degree, while Fig. 5b illustrates the effect of network size on test accuracy. For context, Fig. 6 shows the distribution of degrees selected by different optimizers in one configuration.

I.2 CIFAR-10 Benchmark

First, we present the computational scaling results mentioned in the main text. Similar experiments were conducted on the CIFAR-10 dataset to assess scaling behavior in a more complex image

Table 8: Hyperparameter Grid Search for House Sales Dataset

Model	Hyperparameter	Values Searched
CP-KAN	Max Degree	{5, 7, 9, 11}
	Hidden Size (<code>network_shape</code>)	{20, 32, 64}
	Default Hidden Degree	{3, 5, 7, 9}
	Complexity Weight	{0.0, 0.001, 0.01}
	Learning Rate	{1e-4, 5e-4, 1e-3}
MLP	Depth	{2, 3, 4, 5}
	Hidden Size	{32, 64, 128}
	Dropout Rate	{0.1, 0.2}
	Learning Rate	{1e-4, 1e-3}
	Weight Decay	{0.0, 0.001}
	Batch Size	{64, 128, 256}

Table 9: Hyperparameter Grid Search Definition for Optimization Methods

Method(s) Applied To	Hyperparameter	Values Defined in Grid
QUBO (MNIST, CIFAR-10) IP, Evo, Greedy (MNIST only)	Max Degree	{3, 5, 7}
	Hidden Layers	[64], [128], [32, 32]
	Default Hidden Degree	{3} (Fixed)
	Complexity Weight	{0.01} (Fixed)
	Trainable Coefficients	{True} (Fixed)
	Learning Rate	{0.001, 0.0003, 0.0001}
Evolutionary (MNIST only)	Population Size	{20, 50}
	Generations	{30} (Fixed)

classification task. Fig. 8a shows the relationship between maximum polynomial degree and accuracy, while Fig. 8b illustrates the effect of network size.

The CIFAR-10 results corroborate the findings from MNIST: QUBO optimization facilitates positive scaling with network size, whereas excessively high polynomial degrees can hinder performance. The QUBO solver often selects lower degrees, suggesting the importance of adaptable complexity.

I.3 Forest Coverttype Classification

We also evaluated CP-KAN on the Forest Coverttype dataset, a standard tabular classification benchmark known for requiring models to capture potentially sharp decision boundaries. As detailed in Appendix H, CP-KAN (optimized with QUBO) was compared against an MLP configured for a similar parameter count ($\approx 10k$) and standard baseline models (RandomForest, XGBoost). The results indicated that while CP-KAN achieved reasonable accuracy, it was outperformed by both the MLP and significantly by the tree-based methods. This aligns with the expectation that CP-KAN’s polynomial basis functions are inherently better suited for approximating smooth, continuous functions (as in regression) rather than the potentially discontinuous decision boundaries required for optimal performance on Coverttype. Tree-based models excel in such scenarios by recursively partitioning the feature space. This experiment highlights a limitation of the current CP-KAN architecture for certain types of classification problems, reinforcing its primary strengths in regression and smooth function modeling.

I.4 QUBO Solver Timings

The QUBO optimization step (Phase 1), typically solved via simulated annealing, has a runtime primarily influenced by the number of binary variables in the QUBO matrix (number of neurons $N \times (\max \text{degree } D + 1)$) and the time required to calculate the MSE cost matrix (which depends on the batch size B and input data size). Fig. 7 illustrates the near-linear scaling complexity observed

Table 10: Fixed Training Parameters for KAN/MLP on Covertypes

Parameter	Fixed Value
Epochs	50 (or 500, check script execution)
Batch Size	4096
Learning Rate	1e-3
Optimizer	Adam
Loss Function	CrossEntropy

Table 11: KAN/MLP Configurations Tested on Covertypes (Target Params \approx 10k)

Model	Parameter	Fixed Value
CP-KAN	Network Shape	Determined by calculating summing all the trainable parameters
	Max Degree	10
	Complexity Weight	0.0
	Trainable Coefficients	False
	Skip QUBO for Hidden	False
	Default Hidden Degree	2
MLP	Architecture	Determined by <code>approximate_mlp</code>
	Hidden Activation	ReLU
	Layers include	BatchNorm1d, Dropout

with respect to network size N . To provide concrete examples, Table 13 details the execution time for this QUBO step on the hardware specified in Appendix A.

J Recurrent & Transformer Models (Embedding Trick & Architecture Details)

This appendix provides a reproducible account of how we apply LSTM, GRU, and Transformer models to tabular data using an embedding trick that treats each feature as a “time step” (for LSTM/GRU) or a “token” (for Transformer). We also describe a larger, competition-style GRU variant that was tested.

J.1 Feature-as-Sequence Embedding Trick

For tabular data with D features, standard sequence models expect input shape $[B, \text{seq_len}, \text{input_dim}]$. To adapt tabular data $\mathbf{X} \in \mathbb{R}^{B \times D}$, we first reshape it to $\mathbf{X}' = \mathbf{X}.\text{unsqueeze}(-1) \in \mathbb{R}^{B \times D \times 1}$, treating each feature as a time step or token. Then, we apply a linear layer (e.g., `nn.Linear(1, embed_dim)`) to project this into a higher embedding dimension d_{embed} , resulting in $\mathbf{X}'' \in \mathbb{R}^{B \times D \times d_{\text{embed}}}$. This embedded sequence \mathbf{X}'' is then fed into the LSTM, GRU, or Transformer model. Finally, the model’s output (e.g., the last hidden state for RNNs or pooled tokens for Transformers) is mapped to the target dimension via a final linear layer.

J.2 LSTM and GRU Models

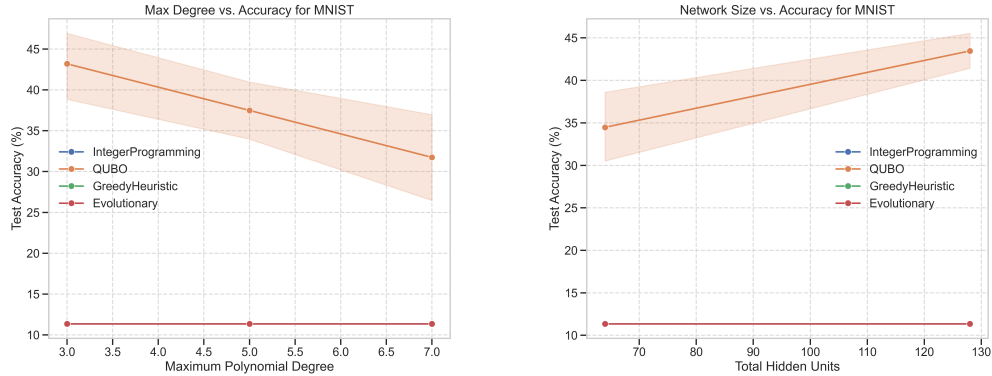
We used standard `torch.nn.LSTM` or `torch.nn.GRU` with `batch_first=True`. Key hyperparameters include hidden dimension d_{hidden} and number of layers N_{layers} . The final hidden state $\mathbf{h}_{\text{final}} \in \mathbb{R}^{B \times d_{\text{hidden}}}$ is passed to a linear layer. We also tested a “competition-style” GRU variant with multiple layers (e.g., $\{500\}$ or $\{250, 150, 150\}$), inter-layer dropout, and a post-GRU feed-forward stack (e.g., $[500, 300]$), inspired by Kaggle solutions but adapted for typical batch sizes.

J.3 Transformer Model (Encoder Only)

Our Transformer encoder approach used `torch.nn.TransformerEncoderLayer` (with model dimension d_{model} , number of heads n_{heads} , feedforward dimension d_{ffn}) stacked into a

Table 12: Baseline Model Configurations for Covertype

Model	Parameter	Fixed Value
RandomForest	n_estimators	100
	random_state	42
	Other	scikit-learn defaults
XGBoost	n_estimators	100
	random_state	42
	use_label_encoder	False
	eval_metric	logloss
	Other	XGBoost defaults



(a) Test accuracy vs. maximum polynomial degree D .

(b) Test accuracy vs. total hidden units.

Figure 5: Impact of model complexity on MNIST test accuracy for CP-KAN solved via QUBO (dashed) and integer programming (solid).

Table 13: Execution time (*mean ± std. dev.* over n runs) for the QUBO optimization step (Phase 1, simulated annealing) on an Apple MacBook Pro (Late 2021, M1 Pro chip) for different CP-KAN layer sizes (N neurons) and maximum Chebyshev degrees (D). Batch size used for MSE calculation was 64.

Layer Size (N)	Degree 3 ($D=3$)	Degree 5 ($D=5$)	Degree 7 ($D=7$)
64	4.35s ± 0.10 (n=5)	6.89s ± 0.17 (n=6)	9.98s ± 0.95 (n=6)
128	8.19s ± 0.02 (n=3)	13.49s ± 0.29 (n=3)	19.17s ± 0.32 (n=3)

`torch.nn.TransformerEncoder` with N_{layers} . After embedding features to $[B, D, d_{\text{model}}]$, the encoder outputs shape $[B, D, d_{\text{model}}]$. We typically average pool across the D tokens before a final linear projection.

J.4 Weighted Loss and Metric

During training, we minimize a weighted MSE (or WMSE) using sample weights w_i , and validate using the competition’s weighted R^2 metric, employing early stopping based on validation R^2 .

J.5 Implementation Notes

Models were implemented in PyTorch. The embedding trick involves `x.unsqueeze(-1)` followed by `nn.Linear`. Standard library modules were used for LSTM, GRU, and Transformer components. Training used the AdamW optimizer, logging the best validation R^2_{weighted} . This feature-as-sequence approach allows applying sequence models to tabular data but requires careful tuning.

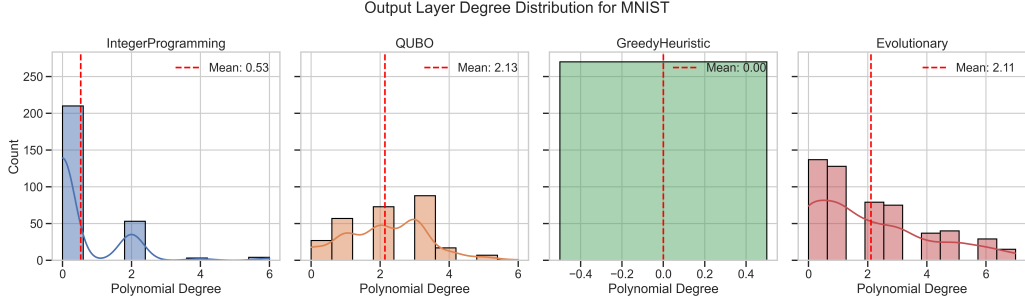


Figure 6: Comparison of polynomial degree distributions selected by different optimization methods for the output layer neurons on the MNIST dataset. This visualization provides context on optimizer behavior and preference for specific degrees.

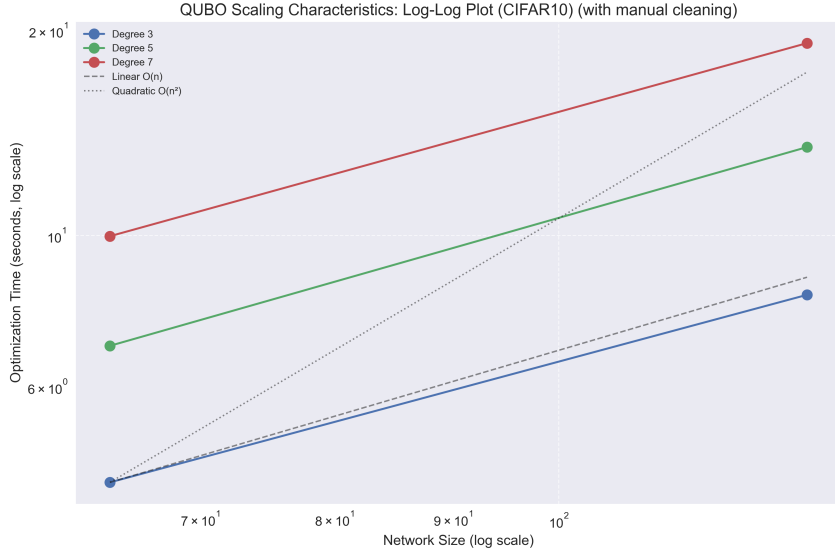
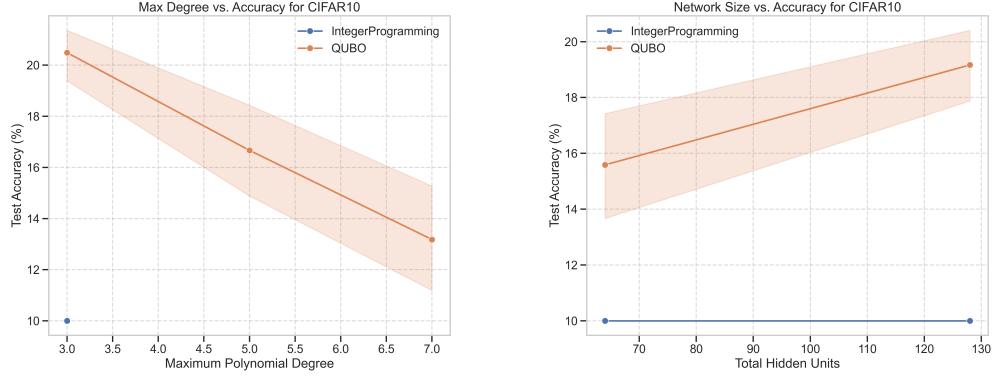


Figure 7: Log-log plot illustrating the computational scaling of the QUBO optimization time versus network size on CIFAR10. Results are shown for different maximum degrees ($D = 3, 5, 7$). The scaling closely follows the linear $O(n)$ reference line, indicating linear complexity. Similar results were observed in the MNIST experiments.

K Theoretical Details for Mean Reversion

This appendix provides the formal statement of the generator decomposition theorem and the error bound related to the Ornstein-Uhlenbeck process discussed in Section 5.

The efficiency of Chebyshev polynomials stems from their approximation properties for smooth functions. Assuming a function $g(x)$ defined on $[-1, 1]$ has k continuous derivatives, its Chebyshev expansion $g(x) \approx \sum_{i=0}^{\infty} c_i T_i(x)$ exhibits coefficients c_i that decay algebraically, typically as $O(i^{-(k+1)})$ [Majidian, 2017]. This rapid decay ensures that smooth functions, like the time-varying transfer function $A_t(\omega)$ in locally stationary processes (after appropriate rescaling of ω), can be accurately approximated using a finite number of Chebyshev terms, underpinning their suitability for CP-KAN.



(a) Test accuracy vs. maximum polynomial degree D .

(b) Test accuracy vs. total hidden units.

Figure 8: Impact of model complexity on CIFAR-10 test accuracy for CP-KAN optimized with QUBO.

Theorem 1 (Generator Decomposition [Applebaum, 2007]). *For the mean-reverting SDE $dX_t = \theta(\mu - X_t) dt + \sigma dW_t$, the infinitesimal generator \mathcal{A} admits a Chebyshev expansion:*

$$\begin{aligned} \mathcal{A}f(x) &= \theta(\mu - x)f'(x) + \frac{1}{2}\sigma^2 f''(x) \\ &= \sum_{n=0}^{\infty} \lambda_n \langle f, T_n \rangle T_n(x), \end{aligned} \quad (13)$$

with $|\lambda_n| \leq C(1 + n^2)$.

This decomposition provides rigorous justification for the use of Chebyshev polynomials in modeling mean-reverting processes often found in finance [Mi, 2016]. Furthermore, for the Ornstein-Uhlenbeck process, tight error bounds can be established for approximations like those potentially learned by CP-KAN [Burtnyak and Malys'ka, 2018]:

$$\mathbb{E}[\|X_t - \hat{X}_t\|^2] \leq C_1 e^{-\theta t} \|X_0 - \mu\|^2 + C_2 \frac{\log d}{d}. \quad (14)$$

Here, \hat{X}_t represents the approximation using polynomials up to degree d . The bound highlights the interplay between the exponential decay due to mean reversion (*heta*) and the approximation error related to the polynomial degree d .